ChemComm

Accepted Manuscript

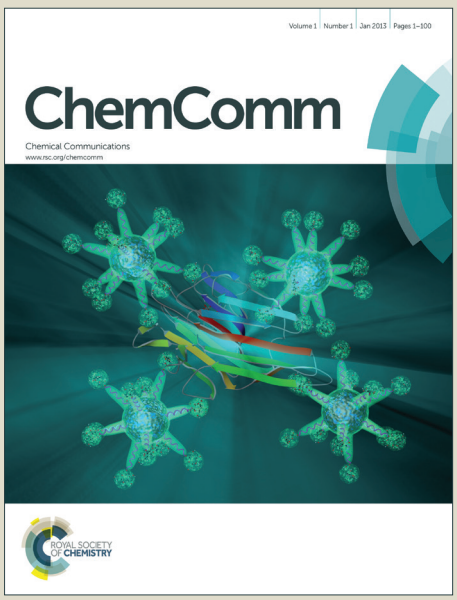

ROYAL SOCIETY OF CHEMISTRY

www.rsc.org/chemcomm

Chem Comm

RSCPublishing

COMMUNICATION

High-Performance Electrocatalyst for Oxygen Evolution Reaction Based on Electrochemical Post-Treatment of Ultrathin Carbon Layer Coated Cobalt Nanoparticles

Cite this: DOI: 10.1039/x0xx00000x

Received 00th January 2012,
Accepted 00th January 2012

DOI: 10.1039/x0xx00000x

www.rsc.org/

Qingqing Xiao, Yuxia Zhang, Xin Guo, Lin Jing, Zhiyu Yang, Yifei Xue, Yi-Ming Yan* and Kening Sun

Electrochemical post-treatment of ultrathin carbon layer coated cobalt nanoparticles generates a novel electrocatalyst, affording a small overpotential of 333 mV at current density of 10 mA cm^{-2} and a small Tafel slope of ~58 mV/decade.

Conversion of solar energy to chemical fuels by photo-induced splitting of water to produce H_2 and O_2 represents a prevailing approach which is both sustainable and environmentally friendly.[1-6] To this end, a stable and efficient catalytic system is commendatory required to efficiently split water, in which the catalytically oxidation of water into molecular oxygen, i.e., oxygen evolution reaction (OER), is a more challenging half reaction.[7-9] Therefore, an effective electrocatalyst is highly desired to expedite the reaction. To date, the oxides of Ru and Ir have been considered to be the best OER catalysts.[10-12] However, these metals are among the rarest and expensive elements on the earth and therefore they are not suitable for practical applications.

Tremendous efforts have been devoted to searching for highly active, durable and low cost OER catalysts. Indeed, notable achievements have been made, including the use of first-row transition metal oxides and perovskites as economic and robust OER electrocatalysts.[5,13-26] Among them, cobalt-based oxides or complexes have shown outstanding performance for OER. Dai et.al.[3] reported the growth of Co_3O_4 nanocrystals on rGO, resulting a high performance OER electrocatalyst. Li et.al.[27] reported Co-Ni layered double hydroxides as efficient OER electrocatalysts in neutral electrolyte.

Different from these works, here we report a novel Co-based OER electrocatalyst by electrochemical post-treatment (ECPT) of the metallic cobalt nanospheres coated with ultrathin carbon layer (Co@C), which is prepared by a facile and controllable chemical deposition method following a simple calcination approach. The ECPT of Co@C (ECPT-Co@C) can effectively in-situ produce cobalt oxides at the surface of cobalt metallic spheres, resulting prominent OER catalytic activity and superior chemical stability, even outperforms commercial IrO_2 and RuO_2.

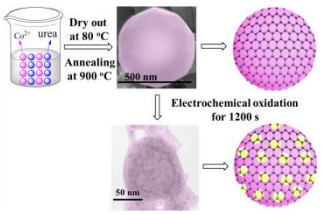

Scheme 1. Schematic illustration of the preparation process of ECPT-Co@C and the complex architecture. Pink and yellow balls correspond to metallic cobalt and CoOx, respectively.

The strategy for the fabrication of ECPT-Co@C is illustrated in Scheme 1. The mixture of urea and $Co(NO_3)_2{\cdot}6H_2O$ was calcined under 900 ^oC and the derived Co@C was further used for electrochemical oxidation to generate ECPT-Co@C. We also calcined $Co(NO_3)_2{\cdot}6H_2O$ under the same conditions and obtained Co-C-0.

For Co@C, well-defined nanoparticles were observed with a diameter of 100-400 nm, as seen in Fig. 1a, proving that the cobalt nanoparticle coated with ultrathin carbon layer has been successfully synthesized. As a comparison, the Co-C-0 was also characterized by scanning electron microscopy (SEM, Fig. S1) and shows uniform spheres with a diameter of ~3 μm, which is about 5 times larger than that of Co@C. It demonstrates strongly that the urea is essentially

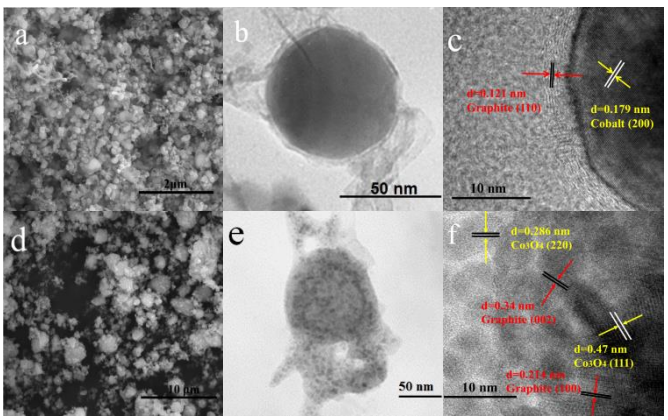

Fig. 1 SEM image of Co@C is shown in (a). TEM and HRTEM images of Co@C are shown in (b) and (c), respectively. SEM image of ECPT-Co@C is shown in (d). TEM and HRTEM images of ECPT-Co@C are shown in (e) and (f), respectively.

necessary for obtaining nanostructured cobalt materials besides functions as carbon source. The transmission electron microscopy (TEM, Fig. 1b) reveals that the thickness of carbon layer is ~10 nm. Some graphite nanosheets were also observed as adhesion to the cobalt nanoparticles. High resolution TEM (HRTEM) of Co@C catalyst (Fig. 1c) shows that the thin carbon layer was strongly covered the cobalt nanoparticles. The lattice fringes of 0.179 nm and 0.121 nm were observed, corresponding to metallic cobalt and graphite, respectively. Fig. 1d displays the SEM image of ECPT-Co@C. Compared to Co@C, no apparent difference in the morphology was observed. However, TEM of ECPT-Co@C (Fig. 1e) reveals very different surface morphology from that of Co@C. It was found that nano-sized particles were decorated uniformly at the surface of ECPT-Co@C, likely being wrapped with the ultrathin carbon layers. These particles were further verified by HRTEM (Fig. 1f), showing that the lattice fringes were 0.286, 0.47 and 0.214, 0.34 nm, corresponding to Co_3O_4 and graphite, respectively. It indicates that the cobalt oxides were produced and closely incorporated into the structure of carbon layer after ECPT.

To investigate the chemical compositions of the Co@C, X-ray diffraction (XRD) characterization was carried out. As shown in Fig. 2a, the typical peaks of 44.2° and 51.5° are corresponding to metallic cobalt while the peak of 26.5° is assigned to graphite, which are in good agreement with the results of HRTEM image. X-ray photoelectron spectrometer (XPS, Fig. 2b) was also applied and shows that only graphite and slight oxygen were detected for Co@C, while no characteristic peaks for cobalt appeared. As XPS is a typical technique probing a few layered atoms at material surfaces, it is reasonable to deduce that the cobalt nanoparticles should be well-coated with ultrathin carbon layer. The mass content of cobalt in Co@C was investigated by inductively coupled plasma-atomic emission spectroscopy (ICP-AES), revealing that the cobalt content is 55.4 wt. %.

Cobalt in high oxidation states have been proposed as the most active sites for OER.[23] Therefore, it is interesting to understand how the metallic cobalt of Co@C was converted to cobalt oxides after ECPT. Indeed, metallic cobalt is more likely to be oxidized (-0.28 V) compared with H_2O (1.23 V). It means that metallic cobalt should be easily converted into cobalt oxides at high potential. Consequently, we deduce that a well-defined OER activity should be attained by ECPTof the Co@C, forming a novel OER electrocatalyst of ECPT-Co@C.

To verify this, we investigated the ECPT-Co@C catalyst by XRD and XPS. As shown in Fig. 2a, the peak intensity of metallic cobalt for ECPT-Co@C clearly decreased, while an obviously new feature peak appears at 34 ° which should be assigned to CoO. We noted that no feature peak for carbon was observed in the XRD pattern of ECPT-Co@C, which should be probably attributed to the blocking effect from the strong peaks of CoO. Furthermore, the XPS (Fig. 2b) of ECPT-Co@C suggests the presence of cobalt oxides, which were confirmed by Co 2p, Co LMM, Co 3s, and Co 3p peaks. Also, the XPS spectra show that the peak intensity of carbon decreased substantially, which is in good agreement with the XRD results. Fig. 2c shows the XPS spectra of Co 2p, revealing the characteristic peaks at 795.6 eV and 780 eV, which are assigned to Co $2p_{1/2}$ and Co $2p_{3/2}$ of Co_3O_4 species. Thus, we conclude that the wrapped metallic cobalt particles were partially converted to cobalt oxides after ECPT and closely incorporated into the structure of the carbon layers at the surface, resulting in a unique nanostructure of carbon layer / cobalt oxides / metallic cobalt. Apparently, such a unique structure has been confirmed by the SEM and TEM images. As the cobalt nanoparticles were broken into smaller nanosized particles after ECPT, the specific area of the catalyst should correspondingly increase. As a consequence, ECPT-Co@C can offer

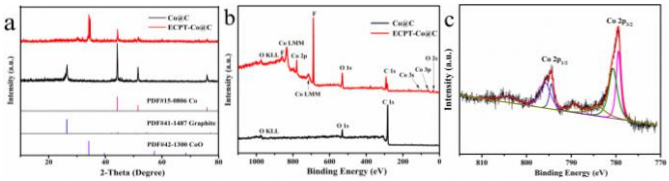

Fig. 2 (a) XRD spectra of Co@C and ECPT-Co@C. (b) XPS spectra of Co@C and ECPT-Co@C. (c) XPS spectra of Co 2p of ECPT-Co@C.

more active sites for OER. In addition, the XPS results inferred that the carbon layers were partially destroyed after ECPT, which would facilitate the diffusion of electrolyte and oxygen gas. Then we can speculate that the ECPT-Co@C would own high activity for OER due to its unique structure and exposed cobalt oxides at the surface.

The electrocatalytic OER activity of ECPT-Co@C was evaluated in 1.0 M KOH solution. The samples were casted on RDE for linear sweep voltammetry (LSV) test (Fig. 3a). Compared with cobalt powder after ECPT (ECPT-Co), ECPT-Co@C exhibits higher current density and lower onset potential, implying the great importance of ultrathin carbon layers. To clearly understand the OER activity of ECPT-Co@C, we also studied Co-C-0, mechanically mixing of cobalt powder and graphite after ECPT (ECPT-Co/Gr), and commercial catalysts of RuO_2 and IrO_2. ECPT-Co/Gr exhibits much lower current intensity compared with ECPT-Co@C, indicating the ECPT of Co/Gr cannot achieve high OER performance. It implies that the special structure of ECPT-Co@C with conductive shell and core is extremely important to achieve enhanced OER activity. Moreover, the poor OER activity of Co-C-0 indicates that the carbon layer was essentially important to the excellent OER activity. We noted that RuO_2 catalyst affords lower onset potential and higher current density at a potential range lower than 1.6 V in comparison to ECPT-Co@C. However, the current density for RuO_2 drops sharply when the potential is higher than 1.6 V, which is far lower than that of ECPT-Co@C. Similarly, ECPT-Co@C catalyst shows better performance than IrO_2. To investigate the intrinsic catalytic activity, OER current was normalized to the surface area of the samples and shown in Fig. S2. Again, ECPT-Co@C shows highest activity. The high OER activity of the ECPT-Co@C was also confirmed by measuring the Tafel slopes (Fig. 3b).The Tafel slope of ECPT-Co@C catalysts was ~58 mV/decade, smaller than that of IrO_2 (~67 mV/decade) and RuO_2 (~85 mV/decade). Moreover, we measured and compared the Tafel plots

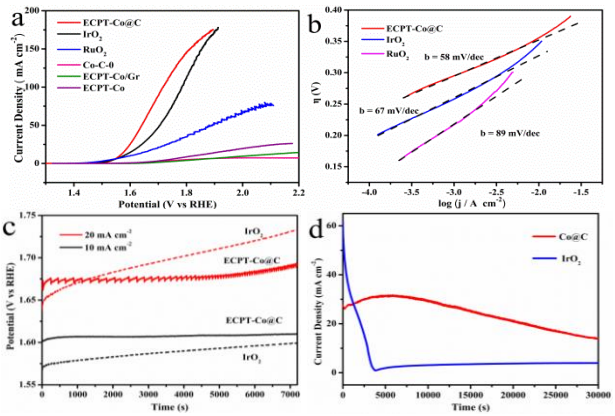

Fig. 3 (a) OER polarization curves for ECPT-Co@C, IrO_2, RuO_2, Co-C-0, ECPT-Co/Gr and ECPT-Co, respectively. (b) Tafel plots of ECPT-Co@C, IrO_2 and RuO_2 derived from (a). (c) Chronopotentiometry curves of RuO_2 and ECPT-Co@C catalyst on RRDE at constant current density of 10 and 20 mA cm^{-2}, respectively. (d) Current profile of Co@C and IrO_2 at 1.62 V.

(Fig. S2) of ECPT-Co@C and RuO_2 in 0.1 M KOH solution. Again, the Tafel slope of ECPT-Co@C catalyst was smaller than that of RuO_2. These results strongly demonstrate that ECPT-Co@C is a promising OER catalyst in alkaline solutions.

Apart from the excellent OER activity, the ECPT-Co@C catalyst also possesses good durability. Fig. 3c shows the chronopotentiometry curves of the samples at an applied current density of 10 and 20 mA cm^{-2}, respectively. No significant change was observed for ECPT-Co@C catalyst, whereas the potential of IrO_2 catalyst increased quickly. We also compared the stability of Co@C and IrO_2 at an applied potential of 1.62 V. By contrast, IrO_2 is far less stable than Co@C, which only 25% of the initial current was lost after 20000 s of continuous operation. The sharp current decreased of IrO_2 may be due to the anodic dissolution under high potential in base.[10] Notably, the current density of Co@C was slowly increased at the first one hour and then decreased because that the metallic cobalt in Co@C catalyst was firstly oxidized and gradually converted into ECPT-Co@C. Thus, we conclude that ECPT of Co@C at constant potential offer an effective method for obtaining high-performance OER catalyst. Unfortunately, although continuous rotating of the working electrode, there were still many bubbles covered on it, leading to the gradually decrease of current density.

We further probe the function of carbon layer of ECPT-Co@C by performing control experiments. ECPT-Co was characterized by XRD（Fig. S3）. It shows the peak intensity of metallic cobalt decreased after ECPT and new features corresponding to CoO appeared, suggesting the metallic cobalt was partially oxidized. However, the ECPT-Co exhibits little OER activity, implying that the promising OER activity for ECPT-Co@C catalyst should contributed from the ultrathin carbon layer, which facilitates the electron transport and thus enhancing the electrochemical kinetics of OER. To verify this, we measured the electron transfer resistance (R_{et}) by performing electrochemical impedance spectroscopy (EIS). Fig. S4 shows the Nyquist plots of cobalt powder and Co@C before and after ECPT. As seen, the cobalt powder exhibits excellent conductivity with a R_{et} of ~1 Ω and that of Co@C catalyst is ~10 Ω. However, huge difference was observed after ECPT in the same condition. The R_{et} of ECPT-Co was greatly increased to ~100 Ω while that of ECPT-Co@C was only ~11 Ω. The results suggest that the ultrathin carbon layer is essentially important to maintain high OER activity of ECPT-Co@C by effectively decreasing the R_{et} of the catalyst. Fig. S5 presents a carton picture, illustrating the role of the unique structure of ECPT-Co@C in achieving favorable OER activity. Three possibilities should be ascribed to the high-performance of ECPT-Co@C towards OER: 1) The in-situ generated ultrathin carbon layer acts as good electrically conductive network, facilitating the electron transport and enhancing the OER activity. 2) The metallic cobalt kernel is a well-conductive support for holding and dispersing the cobalt oxides nanoparticles. 3) A synergic effect between the nano-sized cobalt oxides and the ultrathin carbon layers also possibly contributes to enhancing OER performance. We are currently devoting effort to search more evidence to prove the assumption.

To confirm the gas product, we collected and analyzed it with gas chromatography (Fig. S6). A linear increase of the oxygen amount was observed as the reaction time, indicating the oxygen production rate is constant and the catalysts work very stable. We noted that the product was pure oxygen gas and no CO_2 / CO were detected (Fig. S7 and details in ESI†). Furthermore, the per-metal turnover frequency (TOF) of the catalyst was calculated. Assuming that all the metal sites were involved in the electrochemical reaction, TOF values for ECPT-Co@C catalyst were determined to be 8.8 × 10^{-3}, 0.412, and 1.011 s-1 at η = 300, 450, and 550 mV, respectively. As seen in Table S1, the obtained TOF values for ECPT-Co@C catalyst are comparable to that of some reported cobalt-based catalysts.

In summary, we have reported an ECPT-Co@C as high-performance OER catalyst. The catalyst exhibits promising OER activity and durability towards OER in alkaline solution, even outperforms commercial IrO_2 or RuO_2. The excellent OER performance is attributed to the unique structure of ECPT-Co@C, consisting of electrically conductive metallic cobalt kernel, in-situ generated nano-sized cobalt oxides, and ultrathin carbon layer at the surface as scaffold strongly holding the cobalt oxides. In spite that the onset potential of ECPT-Co@C is higher than that of IrO_2 and RuO_2, the cost-effective, robust, and efficient catalyst is promising in energy storage and conversion technologies. Importantly, our work offers an affordable strategy of rationally design and synthesis of functional materials for a variety of applications.

Notes and references

School of Chemical Engineering and Environment, Beijing Institute of Technology, Beijing, 100081, People's Republic of China.
E-mail: bityanyiming@163.com.

† Electronic Supplementary Information (ESI) available: Experimental details and calculation of TOF. See DOI: 10.1039/c000000x/

1 N. S. Lewis, D. G. Nocera and Proc. Natl, *Acad. Sci.*, 2006, 103, 15729-15735.

2 P. Du and R. Eisenberg, *Energy Environ. Sci.*, 2012, 5, 6012-6021.

3 Y. Liang, Y. Li, H. Wang, J. Zhou, J. Wang, T. Regier and H. Dai, *Nat. Mater.*, 2011, 10, 780-786.

4 M. S. Dresselhaus and I. L. Thomas, *Nature*, 2001, 414, 332-337.

5 L. Trotochaud, J. K. Ranney, K. N. Williams and S. W. Boettcher, *J. Am. Chem. Soc.*, 2012, 134, 17253-17261.

6 S. M. Barnett, K. I. Goldberg and J. M. Mayer, *Nat. Chem.*, 2012, 4, 498-502.

7 M. Garcia-Mota, M. Bajdich, V. Viswanathan, A. Vojvodic, A. T. Bell and J. K. Norskov, *J. Phys. Chem. C*, 2012, 116, 21077-21082.

8 L. Duan, F. Bozoglian, S. Mandal, B. Stewart, T. Privalov and A. Llobet, L. Sun, *Nat. Chem.*, 2012, 4, 418-423.

9 Y. Surendranath, M. W. Kanan and D. G. Nocera, *J. Am. Chem. Soc.*, 2010, 132, 16501-16509.

10 M. G. Walter, E. L. Warren, J. R. McKone, S. W. Boettcher, Q. Mi, E. A. Santori and N. S. Lewis, *Chem. Rev.*, 2010, 110, 6446-6473.

11 Y. Lee, J. Suntivich, K. J. May, E. E. Perry, Y. Shao-Horn, *J. Phys. Chem. Letter.*, 2012, 3, 399-404.

12 M. W. Louie and A. T. Bell, *J. Am. Chem. Soc.*, 2013, 135, 12329-12337.

13 A. J. Esswein, M. J. McMurdo, P. N. Ross, A. T. Bell and T. D. Tilley, *J. Phys. Chem. C.*, 2009, 113, 15068-15072.

14 Y. Li, P. Hasin and Y. Wu, *Adv. Mater.*, 2010, 22, 1926-1929.

15 L. Li and A. Manthiram, *Nano Energy.*, 2014, 9, 94-100.

16 Y. Gorlin and T. F. Jaramillo, *J. Am. Chem. Soc.*, 2010, 132, 13612-13614.

17 B. Cui, H. Lin, J-B. Li, X. Li, J. Yang and J. Tao, *Adv. Funct. Mater.*, 2008, 18, 1440-1447.

18 J. O. Bockris and T. Otagawa, *J. Phys. Chem.*, 1983, 87, 2960-2971.

19 J. Suntivich, K. J. May, H. A. Gasteiger, J. B. Goodenough and Y. Shao-Horn, *Science*, 2011, 334, 1383-1385.

20 L. Li, S.-H. Chai, S. Dai and A. Manthiram, *Energy Environ. Sci.*, 2014, 7, 2630-2636.

21 J. A. Koza, Z. He, A. S. Miller and J. A. Switzer, *Chem. Mater.*, 2012, 24, 3567-3573.
22 J. Esswein, Y. Surendranath, S. Y. Reece and D. G. Nocera, *Energy Environ. Sci.*, 2011, 4, 499-504.
23 B. S. Yeo and A. T. Bell, *J. Am. Chem. Soc.*, 2011, 133, 5587-5593.
24 M.-R. Gao, W.-T. Yao, H.-B. Yao and S.-H. Yu, *J. Am. Chem. Soc.*, 2009, 131, 7486-7487.
25 J. Wu, Y. Xue, X. Yan, W. Yan, Q. Cheng and Y. Xie, *Nano Research.*, 2012, 5, 521-530.
26 J. Masa, W. Xia, I. Sinev, A. Zhao, Z. Sun, S. Grützke, P. Weide, M. Muhler and W. Schuhmann, *Angew. Chem. Int. Ed.*, 2014, 53, 8508-8512.
27 Y. Zhang, B. Cui, C. Zhao, H. Lin and J. Li, *Phys. Chem. Chem. Phys.*, 2013, 15, 7363-7369.

High-Performance Electrocatalyst for Oxygen Evolution Reaction Based on Electrochemical Post-Treatment of Ultrathin Carbon Layer Coated Cobalt Nanoparticles

Qingqing Xiao, Yuxia Zhang, Xin Guo, Lin Jing, Zhiyu Yang, Yifei Xue, Yi-Ming Yan* and Kening Sun

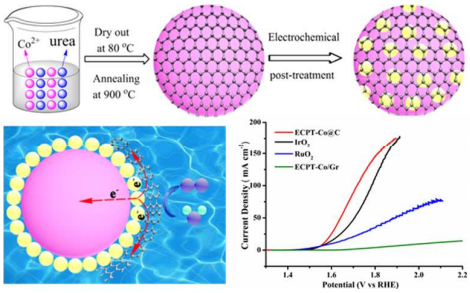

Text: A simple electrochemical post-treatment of metallic cobalt coated ultrathin carbon layer hybrid (Co@C) generates ECPT-Co@C hybrid as a novel OER electrocatalyst with excellent activity.

Table of Content